ELECTROMAGNETIC WAVE DIFFRACTION BY CYLINDRICAL BODIES WITH EDGES

Vladilen N. Vavilov and Eldar I. Veliev
Institute of Radiophysics and Electronics
Ukrainian Academy of Sciences
12 Acad. Proskura Street
Kharkov-85, 310085 Ukraine

ABSTRACT

An accurate numerical-analytical method of solution of the problem of wave diffraction by a perfectly conductive cylindrical body with a cross-section formed by crossing of the "key" elements (such as flat strips and cylindrical screens) is proposed. It is based on the ideas of the moment method and the partial inversion technique of the initial problem operator. For this problem, Gegenbauer polynomials form a complete orthogonal system of the basic functions. As a result, the initial problem is reduced to the solving of infinite systems of linear algebraic equations.

Examples of the flat strip, two crossing cylinders (the cylindrical body with an ogival cross-section) and four quadrangular bodies are studied. Surface current density distributions, total scattering cross sections and radiation patterns are investigated by means of computer calculations.

INTRODUCTION

The scattering of electromagnetic waves by perfectly conducting cylindrical bodies with edges has attracted the notice and interest of investigators both today and in the past. The various methods of solution of such problems effective for the different bands of the dimensions of scatterers (low-frequency, resonant, high frequency) are known. However, in the author's opinion, the two basic approaches of solution of this problem exist today.

The first approach is based on the consideration of the boundary of a cylindrical

Electromagnetics, 13:339–357, 1993

0272-6343/93 $10.00 + .00

body with edges as a single complicated broken contour. One of the basic methods of solving such a problem is reducing it to the solving of the integral equation (I.E.) of the first kind for the current density on the surface of the body. Such an I.E. solution may be arrived at only by numerical techniques (for example, by any version of the moment method (MM)). As a result, the problem is reduced to the solving of the system of linear algebraic equations (S.L.A.E.) [1-3]. If the field singularity near the edges is taken into account analytically and correctly, then the accuracy of the determination of the surface current density is raised significantly [2,3]. In the high-frequency region for the asymptotic solution of this problem, besides techniques based upon the geometrical theory of diffraction (GTD) [4], hybrid methods are used, such as the method based on the combination of the GTD and MM techniques. This was suggested for the solution of diffraction problems on bodies with edges formed by joining flat surfaces [5,6].

Another group of methods of solution is connected with Rayleigh hypothesis [7,8]. In references [7-12], the constructing of solution is based on the possibility of expansion of the unknown scattered field over modal functions. For diffraction of the bodies with limited cross-section these functions are defined as $\Phi_m(p) = H_m^{(1)}(k\rho) \cdot \exp(-im\theta)$, $m = 0, \pm 1$; $p = p(\rho, \theta)$, or as a plane wave for the scattering by grating. However, for the scatterers with a complex boundary or with edge points the Rayleigh series can diverge, as several authors note [7,8]. Using the smoothing procedure for bodies with complicated boundary of scatterers and the singular-smoothing procedure for bodies with several edge points, further developments of the conventional mode-matching method are fulfilled [9,12]. But, as noted, the present algorithms are not general, since they are restricted by the number of the edge points.

The main principle of the second approach is the consideration of the cylindrical body as a composite body formed by the junction ("gluing") of "key" elements together. Every such element is a separate body facet. In this case, the problem of wave diffraction by a polygonal cylindrical body (PCB) is similar to one by N bodies. As a result, the scattered field may be represented as a superposition of fields scattered by each facet of the body (i.e., in the form of the superposition of fields excited by a corresponding surface current on the facets). The flat strip is often used as such a "key" element [13]. The diffraction problem by polygonal cylinders with a cross-section formed by crossing the straight line segments is considered in reference [14].

In this paper, we suggest an effective numerical-analytical method of solution to the problem of diffraction by sufficiently wide class of complicated two-dimensional scatterers. The contours of cross-sections of such structures are formed by superposition of the segments of straight line and the circular arcs. This method is a variety of the boundary I.E. one and belongs to the second approach introduced previously. The application of the Fourier transform (integral, in the case of a flat facet, and discrete, in the case of a circular arc facet) to the unknown function of surface current density is the main condition of such a technique. As a result, the coupled dual integral or series equations are reduced to the solution of Fredholm's type S.L.A.E. The restriction of such method is the necessity of the equality of angles in the apexes of the cross-section contour. New accurate solutions of the wave diffraction problem by flat strips and circular arcs are contained in this method.

1.FORMULATION OF THE PROBLEM

Consider a two-dimensional, perfectly conducting cylindrical body with edges as shown in Fig.1. The body's cross-section, defined by contour L has a finite number (N) of convex edge points. The contour part between the two neighboring edge points (q and $q+1$) is designated as L_q ($q = 1, \dots, N$). This contour is either a straight line or a circular arc. The angles between the tangential vectors at the edges of the scatterer defined in the exterior are equal β_q ($q = 1, \dots, N$). In this paper we consider the case:

$$\beta_1 = \beta_2 = \cdots = \beta_N = \beta$$

Introduce the parameter $\nu = \dfrac{\pi}{\beta}$. In the case of the convex edge point contour this, parameter belongs to the interval [1/2,1].

The E-polarized plane wave $E_z^i(x,y) = e^{ik(\alpha_0 x + \beta_0 y)}$, where $\beta = \cos\varphi_0$, $\alpha_0 = \sin\varphi_0$, $k = \dfrac{2\pi}{\lambda}$ - and λ = a wave-length, is incident from the angle φ_0. The angle of incidence is arbitrary. An $\exp(-iwt)$ dependence is assumed and suppressed throughout. The determination of the scattered field is reduced to the solution of the scalar Helmholtz equation, which must be complemented by a Sommerfeld radiation condition, by Direchlet's boundary condition (C2) at the surface of the cylindrical body, and by Miexner's edge condition (C3).

Applying the second Green's formula for functions satisfying conditions C2 and C3, we can write the following integral presentation for $E_z^{tot}(p)$:

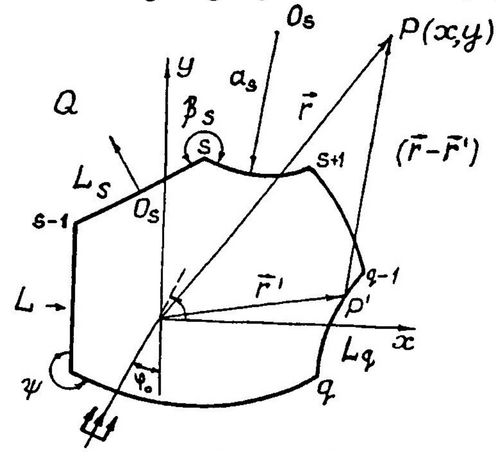

Fig.1. Geometry of problem (illustrated for a complicated cylindrical body).

$$E_z^{tot}(p) = -\oint_L \frac{\partial}{\partial \vec{n}'} E_z^{tot}(p') G(p,p') dl + E_z^i(p) \tag{1}$$

where $\vec{n}'$ is the exterior normal to the contour L, p' = the point on the L and $G(p,p')$ = the two-dimensional free space Green's function. It has been shown, that the function $\rho(p) \equiv \frac{\partial}{\partial \vec{n}'} E_z^{tot}(p)$ coincides (with factor accuracy) with the current density function on the surface of the scatterer.

Using the idea of the second approach, we consider the geometry of the scattering body with contour L as superposition of the ordinary scatterers with contours L_s $(s = 1, \ldots, N)$ having joint points. The total field can be written as

$$E_z^{tot}(p) = -\sum_{s=1}^{N} \int_{L_s} \rho^s(p_s') G(p, p_s') dl_s + E_z^i(p) \tag{2}$$

where $\rho^s(p_s')$ is the unknown surface current density function.

For definition of the functions $\rho^s(p_s')$ the total field must satisfy condition C2:

$$\left(E_z^i(p) + \sum_{s=1}^{N} E_z^s(p) \right) \Bigg|_L = 0 \qquad p \in L, \qquad L = \bigcup_{s=1}^{N} L_s \tag{3}$$

Consequently, to satisfy C2 on every facet, it is necessary to write fields $E_z^i(p)$ and $E_z^q(p)$, $(q = 1, \dots, N)$ at the chosen local coordinate system connected with facet number s, $(s = 1, \dots, N)$. Picking out the field $E_z^s(p)$ scattered by the S facet of the body from the common number of the item, we obtain N coupled I.E. of the first kind relatively of unknown functions, $\rho^s(p_s')$:

$$\int_{L_s} \rho^s(p_s')G(p_{ss}, p_s')dl_s + \sum_{q=1,(q\neq s)}^{N} \int_{L_q} \rho^q(p_q')G(p_{qs}, p_q')dl_q = E_z^i(p_{ss}), \quad s = 1, \dots, N. \tag{4}$$

The following definitions are introduced here:

p_s' - the point of integration on the contour L_s;

p_{ss} - the L_s contour point at the $X_sO_sY_s$ coordinate system;

p_{qs} - the same contour point, but at the $X_qO_qY_q$ coordinates system;

p_q' - the point of integration on the contour L_q (see Fig.2).

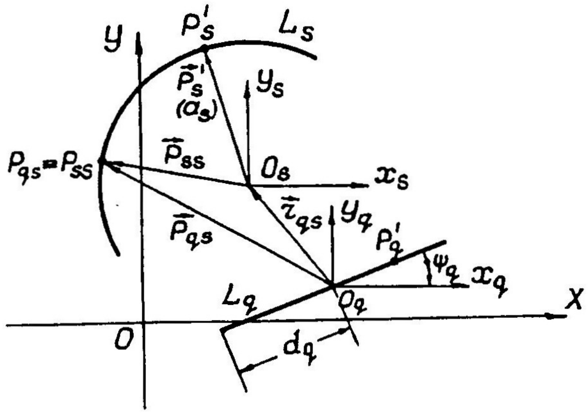

Fig.2. Illustration for determination of a operator D_q^s.

Introduce:

(a) the operator of the fulfillment of boundary condition C2 on the s facet for the field scattered by q facet of the body:

$$D_q^s[\rho^q(p_q')] = \frac{i}{4}\int_{L_q} \rho^q(p_q')H_0^{(1)}(k|\vec{p}_{qs} - \vec{p}_q'|)dl_q, \quad q = 1, \dots, N; \quad s = 1, \dots, N; \tag{5}$$

where $\vec{p}_{qs}$ = radius-vector corresponding to the point p_{qs} on L_s and $\vec{p}_q'$ = radius-vector corresponding to the point p_q' on L_q.

(b) the Fourier presentation operator of the surface current density function $\rho^s(p'_s)$ determined on the interval $p'_s \in L_s$ and added by zero outside this one:

$$F_s[\rho^s(p'_s)] = \begin{cases} \frac{1}{2\pi} \int\limits_{-\infty}^{\infty} g^s(\alpha) e^{ikd_s \cdot \alpha \eta'_s} d\alpha; & \eta'_s = \frac{x'_s}{d_s} \quad \text{—straight line} \\ \frac{2}{i\pi a_s} \sum\limits_{(m)} \rho^s_m e^{in\theta_s \eta'_s}; & \eta'_s = \frac{\varphi'_s}{\theta_s}; \quad \text{—circular arc}. \end{cases} \tag{6}$$

Applying the integral and discrete presentations of the Hankel function $H_0^{(1)}$ $(k\,|\vec{p} - \vec{p'}|)$ [18], and the expression (6), we find the operator in the explicit form:

$$D^s_s[\rho^s(p'_s)] = \begin{cases} \int\limits_{-\infty}^{\infty} g^s(\alpha) K_s(\alpha) e^{ikd_s \cdot \alpha \eta'_s} d\alpha; & K_s(\alpha) = \frac{1}{\sqrt{1-\alpha^2}}; \\ \sum\limits_{(m)} \rho^s_m K^s_m e^{in\theta_s \eta'_s}; & K^s_m = J_m(ka_s) H^{(1)}_m(ka_s). \end{cases} \tag{7}$$

Writing equations (4) in operator form and completing it by the condition of the zero equality of the functions $\rho^s(p'_s)$ outside the contours L_s $(s = 1, \dots, N)$, we receive the connected system of dual (integral or series) equations $D(I,S)E$:

$$\begin{cases} D^s_s[\rho^s(\eta'_s)] = E^i_z(\eta_s) + \sum\limits_{q=1, q\neq s}^{N} D^s_q[\rho^s(\eta'_s)], & |\eta_s| < 1, \\ F_s[\rho^s(\eta_s)] = 0, & |\eta_s| > 1, \end{cases} \tag{8}$$

where we have used the passage $p_{ss} \to \eta_s$ $p'_s \to \eta'_s$.

Finnaly, we write the expression for the field scattered by L_s body facet:

$$E^s_z(p_s) = \begin{cases} \frac{i}{4\pi} \int\limits_{-\infty}^{\infty} g^s(\alpha) e^{ik(x_s \alpha + y_s \sqrt{1-\alpha^2})} \frac{d\alpha}{\sqrt{1-\alpha^2}}, & y_s \geq 0, \quad p_s = p(x_s, y_s) \\ \sum\limits_{m=-\infty}^{\infty} \rho^s_m \begin{Bmatrix} J_m(ka_s) H^{(1)}_m(kr_s) \\ J_m(kr_s) H^{(1)}_m(ka_s) \end{Bmatrix} e^{im\varphi_s}, & \begin{matrix} a_s < r_s \\ a_s \geq r_s \end{matrix}; \; p_s = p(r_s, \varphi_s). \end{cases} \tag{9}$$

2. THE METHOD OF SOLUTION FOR $D(I,S)E$ (8).

For suggested method clearness we consider the simplified system $D(I,S)E$, the analogical system (8), with the arbitrary right-hand part $f(\eta)$ (index s is omitted):

$$\begin{cases} D[\rho(\eta')] = f(\eta), & |\eta| < 1, \\ F[\rho(\eta)] = 0, & |\eta| < 1. \end{cases} \tag{10}$$

Introduce the next system of definition:

$$\varepsilon = \begin{cases} kd & (A) \\ \theta, & (B) \end{cases}; \quad \xi = \begin{cases} \alpha \\ m \end{cases}; \quad e(\xi) = \begin{cases} g(\alpha) \\ \rho_m \end{cases}; \quad \gamma(\xi) = \begin{cases} K(\alpha) \\ K_m \end{cases}. \tag{11}$$

Here $e(\xi)$ is the Fourier transform (integral or discrete) for function $\rho(\eta)$ in (10). Using (11) and introducing the operator $\hat{A}(\xi)$ as:

$$\hat{A}(\xi) = \left\{ \int_{-\infty}^{\infty} \ldots d\xi(A) \text{ or } \sum_{\xi=-\infty}^{\infty} \ldots (B) \right\}$$

we can write the system (10) as follows:

$$\begin{cases} \hat{A}(\xi)[e(\xi)\gamma(\xi)e^{i\varepsilon\xi\eta}] = f(\eta), & |\eta| \leq 1; \\ \hat{A}(\xi)[e(\xi)e^{i\varepsilon\xi\eta}] = 0, & |\eta| > 1; \end{cases} \tag{12}$$

The unknowns $e(\xi)$ as follows from condition $C3$, belong to the space $\tilde{L}_2$ defined as $\tilde{L}_2 \left\{ e(\xi) : \hat{A}(\xi)[|e(\xi)|^2(1+|\xi|)^{-1}] < \infty \right\}$. The thrigonometrical functions are a kernel of such equations as (8). We investigate system (12) with following assumptions:

(a) The following expression for the function $\rho(\eta)$ takes place:

$$\rho(\eta) = \begin{cases} (1-\eta^2)^{\nu-1} \cdot \varphi(\eta), & \eta \in [-1,1], \quad \nu \geq \frac{1}{2} \\ 0, & \eta \notin [-1,1], \end{cases} \tag{13}$$

where $\varphi(\eta)$ is a continuous function belonging to the space $L_2^{\nu-1}[-1,1;\ (1-\eta^2)^{\nu-1}]$, which is the space of regular functions with a scalar product of weight factor $(1-\eta^2)^{\nu-1}$ [16]. The singularity of the field near the edge is taken into account in (13) analytically.

(b) The value $\gamma(\xi)$ may be written in the form

$$\gamma(\xi) = \frac{c}{|\xi|}(1-\delta(\xi)), \qquad \delta(\xi) \underset{\xi\to\infty}{\sim} (\xi^{-1-\tau}), \qquad 0 < \tau \leq 1 \tag{14}$$

where C is a constant.

(c) The function $f(\eta)$ is continuous and its derivative belongs to the space $L_2^{\nu-1}$.

Since the continuous function $\varphi(\eta)$ belongs to the space $L_2^{\nu-1}$, in which the Gegenbauer polynomials $\{C_n^{\nu-1/2}(\eta)\}_{n=0}^{\infty}$ form a basis, $\varphi(\eta)$ can be expanded in a uniformly converging series for these polynomials. According to (13), we can write

$$\rho(\eta) = (1-\eta^2)^{\nu-1} \sum_{n=0}^{\infty} x_n C_n^{\nu-1/2}(\eta), \qquad \nu \geq 1/2 \tag{15}$$

where $\{x_n\}_{n=0}^{\infty}$ are unknown coefficients.

Having used the expansion (15), we obtain the representation of the Fourier coefficients $\{e(\xi)\}_{\xi=-\infty}^{\infty}$ for the function $\rho(\eta)$:

$$e(\xi) = \frac{\varepsilon \cdot 2^{1-2\nu}}{\Gamma(\nu-1/2)} \sum_{n=0}^{\infty} (-i)^n x_n \beta_n \hat{J}_{n+\nu-1/2}(\varepsilon \cdot \xi). \tag{16}$$

The connection in (16) between $e(\xi)$ and x_n allows us to show that the homogeneous equation in (10) is satisfied identically.

To determine the unknown $\{x_n\}_{n=0}^{\infty}$, we substitute the representation (16) into (12). Using the expansions of $f(\eta)$ and $e^{i\varepsilon\xi\eta}$ for the Gegenbauer polynomial series, we obtain the following infinite system of linear algebraic equations (S.L.A.E.) for $\{x_n\}_{n=0}^{\infty}$:

$$\sum_{n=0}^{\infty} (-i)^n x_n \beta_n [Q_{k,n} - L_{k,n}] = \Gamma_k, \qquad k = 0, 1, 2, \dots \tag{17}$$

where

$$\beta_n = \frac{\Gamma(n+2\nu-1)}{\Gamma(n+1)}; \hat{J}_{n+\nu-1/2}(x) = \frac{J_{n+\nu-1/2}(x)}{(x/2)^{\nu-1/2}};$$

$$f(\eta) = \sum_{k=0}^{\infty} f_k C_k^{\nu-1/2}(\eta); \qquad \gamma = \frac{2^{2\nu-1} \cdot f_k}{\varepsilon \cdot i^k (k+\nu-1/2)}$$

The specific form of the matrix elements $\{Q_{k,n}\}_{k,n=0}^{\infty}$ and $\{L_{k,n}\}_{k,n=0}^{\infty}$ depends upon the form of the contour L_s $(s = 1, \dots, N)$ [14, 16]. It is important, that the matrix elements $\{Q_{k,n}\}_{k,n=0}^{\infty}$ can be calculated analytically and the others, i.e., $\{L_{k,n}\}_{k,n=0}^{\infty}$, $\{\Gamma_k\}_{k=0}^{\infty}$, only numerically. The infinite S.L.A.E. (17) belongs to the class of operator equations for which Fredholm's alternative is valid. The approximate solution of the system may be obtained with any desired accuracy by truncation.

3. THE SOLUTION OF THE PROBLEM

Using the solution of the system (17), we receive the infinite S.L.A.E. for the unknown coefficients

$$\sum_{n=0}^{\infty} x_n^s [A_{k,n}^s + B_{k,n}^s] + \sum_{q=1,q\neq s}^{N} \sum_{p=0}^{\infty} x_p^q M_{k,p}^{qs} = \Gamma_k^s, \qquad k = 0, 1, 2, \dots \qquad (18)$$

where the matrix elements $\{A_{k,n}^s\}_{k,n=0}^{\infty}$ and $\{B_{k,n}^s\}_{k,n=0}^{\infty}$ are connected with $\{Q_{k,n}^s\}_{k,n=0}^{\infty}$ and $\{L_{k,n}^s\}_{k,n=0}^{\infty}$, respectively. The matrix operator M^{qs} defines the value and character of the interaction between the facets with number q and s. Specific expression of the $\{M_{k,n}^{qs}\}_{k,n=0}^{\infty}$ is cumbrous and has been omitted. It is calculated only numerically [14, 16].

4. NUMERICAL RESULTS AND COMPARISON

The first stage of numerical experiments based on the developed calculative algorithms studies the investigation of the efficiency of the suggested method. The solutions of the diffraction problems for such "key" scatterers as circular cylindrical screen and flat strip were obtained.

For a cylindrical screen, the comparative analysis of this method with other methods previously proposed (for example, the method of the Riemann-Hilbert problem (R. -H.P.) [17]) was carried out for both polarization cases. The absolute values of the surface current density (E-pol case) $|\rho(\eta)|$ calculated by both proposed method and the R. -H.P. method are shown in Fig.3. Noticeable differences both in the behavior of the functions $|\rho(\eta)|$ and in its absolute values take place. The biggest deflections of the current functions arrive above 40 per cents. The surface current density calculation using (15) is more effective. This is connected with availability of the weight factor, which takes into account the character of the singularity of the function $|\rho(\eta)|$ near the edges ($\eta = \pm 1$) and more rapid convergence of the series. Comparison of the obtained results with ones received by Ziolkovski *at al.* [17], where authors fulfilled the improvement of convergence of the Fourier series, gives a good agreement. In the H-pol case (Fig.4), the absolute values of the surface current density practically coincide for both cases. The Fig.5 shows the azimuthal components for the light and shadow regions of the flat strip (E-pol).

The second stage studies the investigation of the E-pol scattering by a cylindrical body with complicated cross-section. Mainly attention is paid to the problem of plane wave diffraction by a body with an ogival cross-section (Fig.6). This structure, formed by "gluing" the two circular arcs L_s with different radii a_s and extents θ_s is the simplest one which can be studied by the suggested method. What's more, the possibility of change in the field singularity near the edge points exists. The obtained results were compared with the results of wave diffraction on canonical scatterers, such as a flat strip and a circular cylinder.

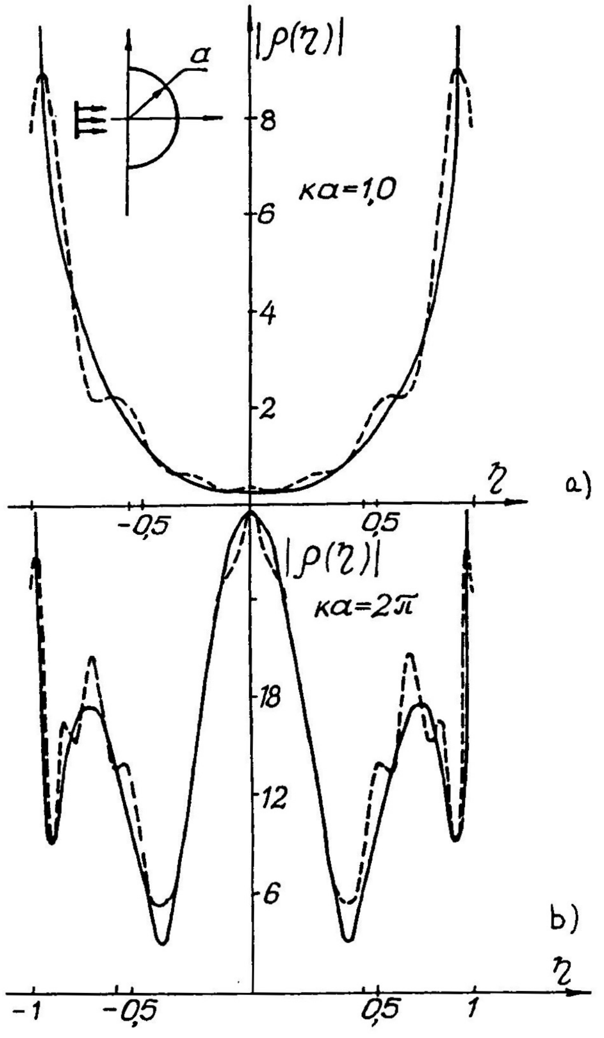

Fig.3. Magnitude of current density induced on the cylindrical screen (E-pol).

a) $ka = 1$, b) $ka = 2\pi$ and $\theta = 90^o$, $\varphi_0 = 90^o$.

For computations of the total scattering cross section (TSCS) σ_s^E and radiation pattern (RF) $|F^E(\varphi)|$ of the scattered field, the following formulas are applied:

$$\sigma_s^E = \frac{1}{ka_1}\sum_{(m)}|\hat{\rho}_m|^2; \qquad \hat{\rho}_m = \sum_{q=1}^{N}\sum_{(p)}\rho_p^q J(ka_q)J_{p-m}(kr_{qs})e^{i(p-m)\varphi_{qs}};$$

$$|F^E(\varphi)| = \left|\sum_{q=1}^{N} e^{ikr_{oq}\cos(\varphi-\varphi_{oq})}\sum_{(m)}\rho_m^q J_m(ka_q)e^{im(\varphi-\pi/2)}\right|;$$

where r_{oq} and φ_{oq} are the coordinates of the origin Oq in the selected system, usually connected with cylinder number 1. Using expressions (16) and (15), we can calculate the Fourier coefficients and the surface current density $\rho(\eta)$ (the azimuthal component $|H_\varphi(\eta)|$), respectively.

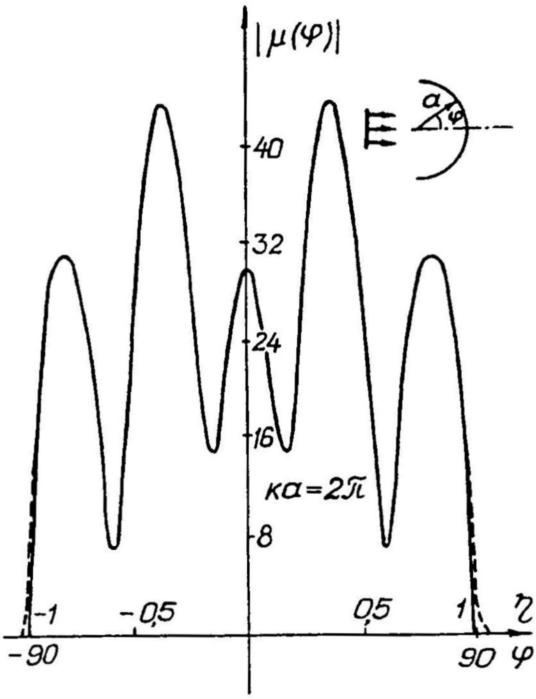

Fig.4. Magnitude of current density induced on the cylindrical screen (H-pol). $ka = 2\pi$, $\theta = 90^o$ and $\varphi_0 = 90^o$.

The frequency dependencies of the σ_S^E for the plane wave incidence 0^o and 90^o are plotted in Fig. 6.

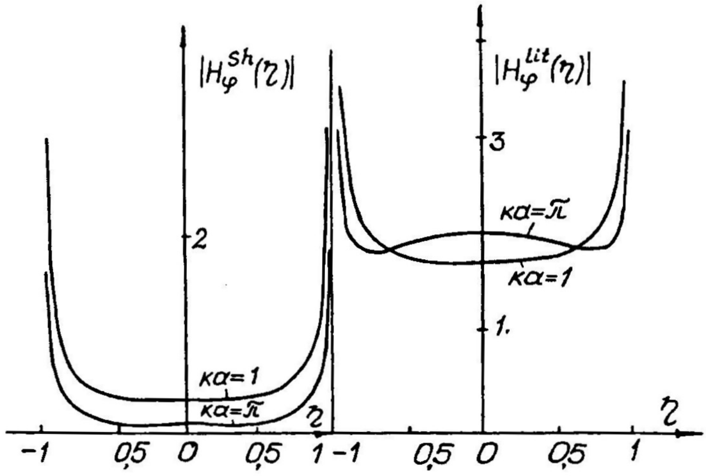

Fig.5. Normalized magnitude of azimuthal component $|H_\varphi(\eta)|$ for flat strip on the light and shadow regions. $kd = 1$ and π, $\varphi_0 = 90^o$.

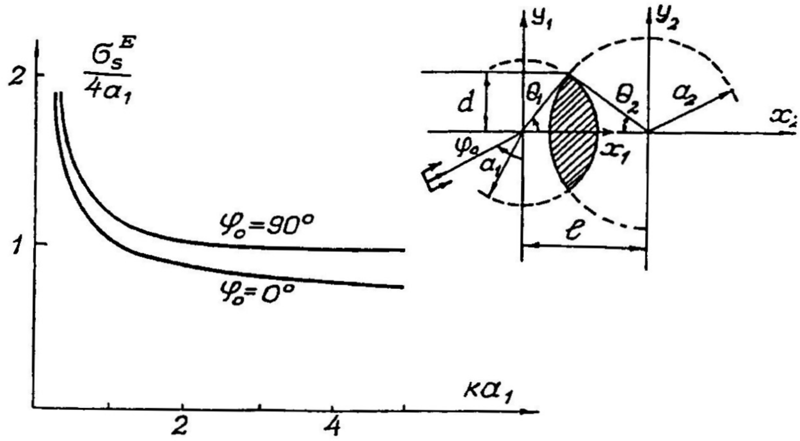

Fig.6. Total SCS for ogival cylinder. $a_2/a_1 = 1$, $l/a_1 = 1$, $\theta_{1,2} = 60^o$, $\varphi_0 = 0^o$ and $\varphi_0 = 90^o$.

Fig.7 represents the RP change due to the change of the cross-section shape of the body at the fixed incidence angle $\varphi_0 = 90^o$ (the transient dimensions equal λ and 2λ, respectively). Also, the RP for the flat strip (solid line) and the circular cylinder (dashed line) are represented in Fig.7 (upper part).

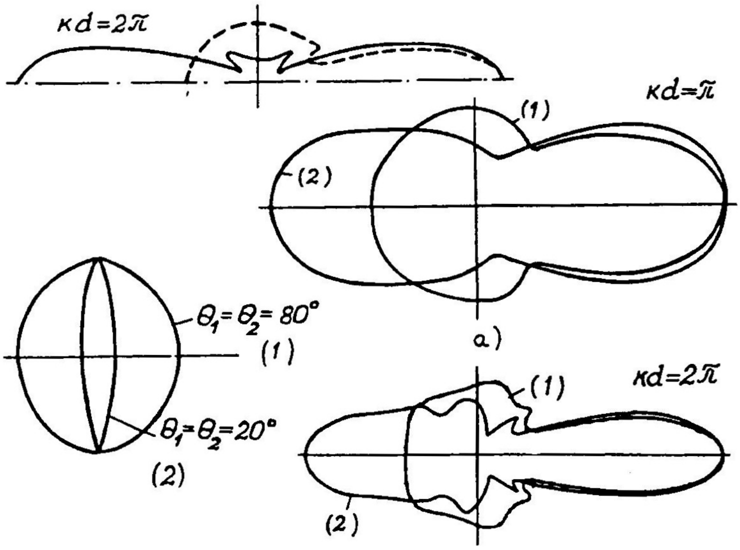

Fig.7. RP for ogival cylinder ((1) - $\theta_{1,2} = 80^o$, (2) - $\theta_{1,2} = 20^o$) and for flat strip (solid line) and circular cylinder (dashed line) in the upper part ($kd = 2\pi$). a) $kd = \pi$, b) $kd = 2\pi$ and $\varphi_0 = 90^o$.

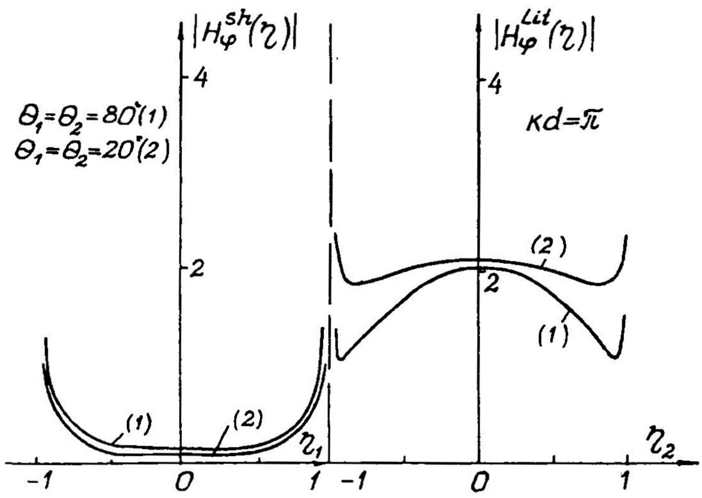

Fig.8. Normalized magnitude of azimuthal component $|H_\varphi(\eta)|$ for ogival cylinder. $\varphi_0 = 90^o$.

With decreasing of the values $\theta_{1,2}$ (in this case $\theta_1 = \theta_2$), the shape of the cross-section draws nearer the flat strip. The back lobe becomes longer. The main lobe does not change practically. Fig.8 shows the $|H_\varphi(\eta)|$ distributions on the light and shadow facets of the body. When the body shape approaches the flat strip, the values $|H_\varphi(\eta)|$ on both facets approximate to the corresponding characteristics for the flat strip. When the cross-section is increased and draws nearer to the shape of the circular cylinder, the current on the light facet is decreased and its distribution character is changed and resembles the facet shape. Excluding the edge points, the current on the shadow region is practically constant.

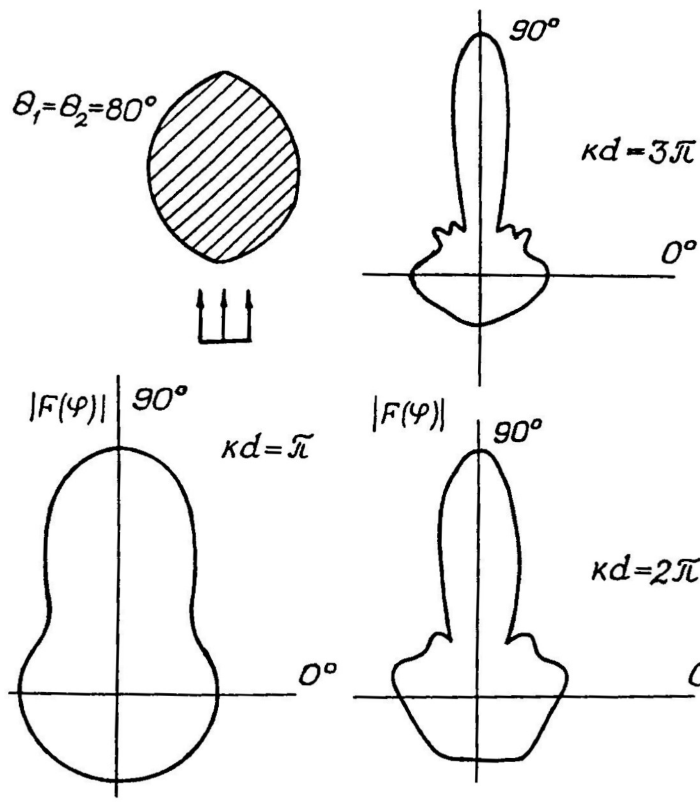

Fig.9. RP for ogival cylinder. $\theta_{1,2} = 80^o$ and $\varphi_0 = 0^o$ ($kd = \pi \div 3\pi$).

Consider another cases of the plane wave incidence. If the extent angles $\theta_{1,2}$ equal 80^o and the incidence angle is changed, the main lode of RP does not practically change at the fixed frequency parameter $kd = \pi, 2\pi$ and 3π. The side radiation shape is not significantly changed (more noticeably for the cases $kd = 2\pi, 3\pi$). For three value kd and the incidence angle $\varphi = 0^o$ the RP are presented in the Fig.9.

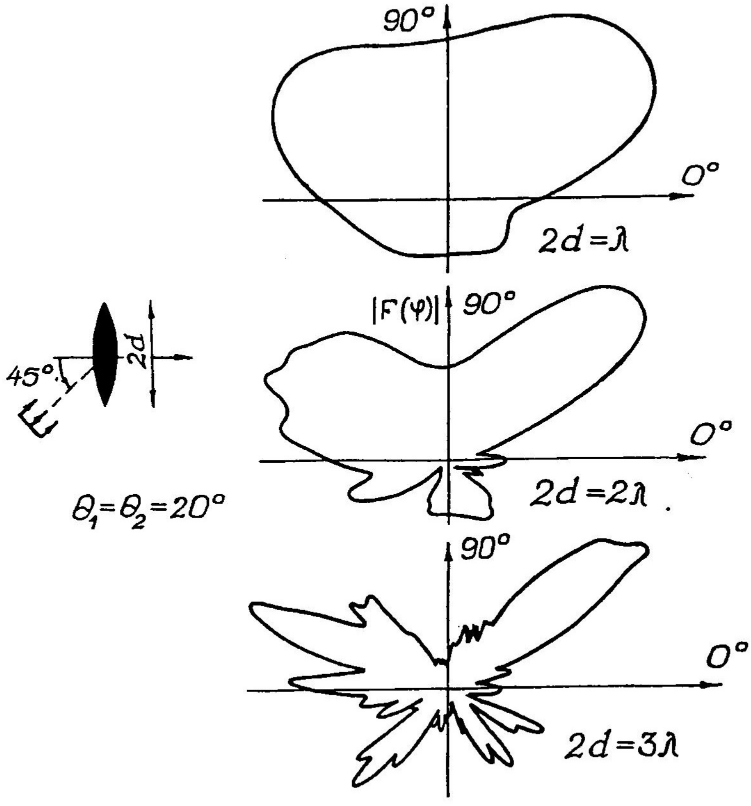

Fig.10. RP for ogival cylinder. $\theta_{1,2} = 20^o$ and $\varphi_0 = 45^o$ $(kd = \pi \div 3\pi)$.

The analogous calculations were fulfilled for the other extent angles. For $\theta_{1,2} = 45^o$ the dependence of the RP shape from incidence angle becomes more visible. When the body shape approaches the flat strip ($\theta_{1,2} = 20^o$), then this dependence is significant, especially with the increasing of the frequency parameter. For example, the RP change at the change of kd from π to 3π is shown in Fig.10. We see that the RP is modified noticeably, but that some of its main features (the directions of the main and the basic side lobes) are kept, although the lobes are narrowed and become more broken. Fig.11 shows the smooth change of the surface current density from the maximum on the light region to the minimum on the shadow one.

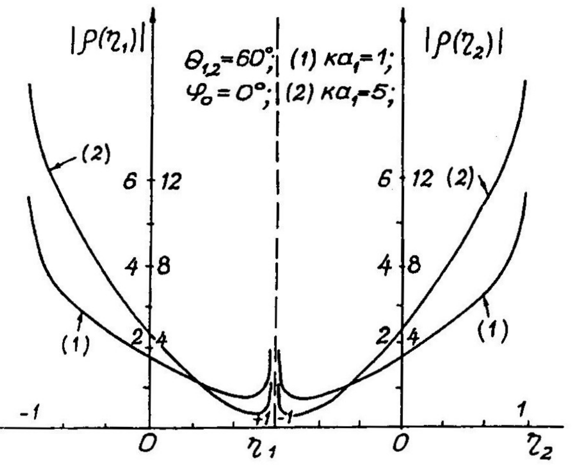

Fig. 11. Magnitude of current density induced on the ogival cylinder.

The change of the RP at the change of the shadow facet shape (the light part of the body remains the same) is also studied (Fig. 12). At the gradual decrease of the extent angle θ_1 of the shadow region from $\theta_1 = 80^o$ to 20^o, the main RP lobe is negligibly widened. The back lobe becomes longer. However, its change is insignificant at $\theta_1 = 40^o$. In this situation the shadow facet of the body does not influence the RP shape.

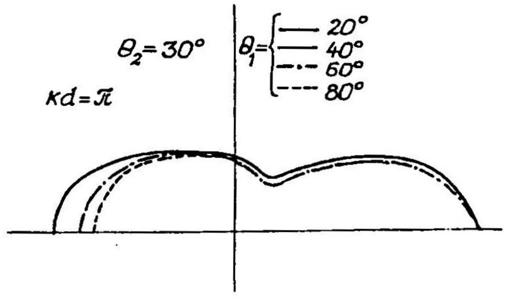

Fig.12. RP for ogival cylinder with variable shadow facet. $\varphi_0 = 90^o$, $\theta_2 = 30^o$ and $\theta_1 = 20^o$-80^o.

The RPs of the scattered field at the two wave incidence angles for the scatterer formed by crossing the four circular arcs are plotted in Fig.13. For the case of $\varphi_0 = 90^o$, the RP has main and back lobes only. Another situation takes place in the case of $\varphi_0 = 90^o$. The back lobe becomes insignificant (5 times smaller than the main lobe).

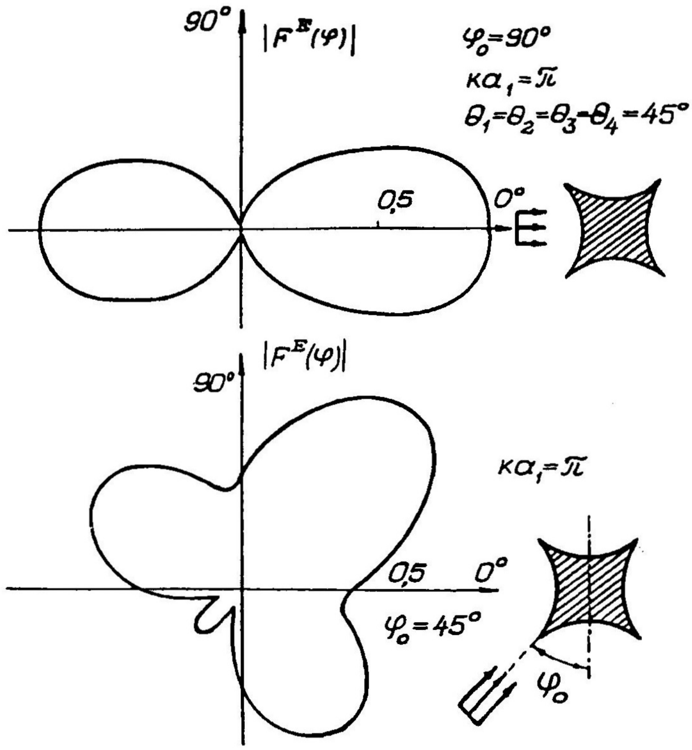

Fig.13. RP quadrangular cylinder.

It is necessary to note that the suggested method of solution allows us to investigate the dependencies σ_s^E, RP and $|H_\varphi(\eta)|$ at the change of the parameter ν in the limits from 1/2 to 1. The complete numerical analysis shows that

a) σ_s^E and RP do not practically change;

b) the change of the values of the component $|H_\varphi(\eta)|$ does not compose more than 1-3 per cent in the interval $\eta \in [-1,1]$.

This fact tells us that the accuracy of taking into account the field behavior near the edge points of a body is not significant for the far field calculation, and it is necessary only for calculation of such data as ohmic loses.

CONCLUSION

A hybrid MM and partial inversion technique has been applied in this paper to treat the problem of electromagnetic diffraction on a cylindrical body with edges. Use of the Gegenbaur polynoimials leads to the evident taking into account of field singularities near the edge points of the body. The efficiency of this technique for the resonance case has been demonstrated. The scattering problem discussed here is important not only for the theory of diffraction, but also for the open resonator theory and for the antenna applications.

ACKNOWLEDGEMENT

The authors are grateful to Vladimir V.Veremey for his aid, discussion, and suggestion.

REFERENCES

1. Mei, K.K. and J.G.Van Bladle, "Scattering by perfectly conducting rectangular cylinders", *IEEE Trans.*, vol.AP-11, no.2,.pp.183-193,1963.
2. Abdelmessih, S. and G.Sinclar, "Treatment of singularities in scattering from perfectly conducting polygonal cylinders - a numerical technique", *Can. Jour. Phys.*, vol. 45, no.3, pp.1305-1319, 1967.
3. Hunter, J.D., "Surface current density on perfectly conducting polygonal cylinders", *Can. Jour. Phys.*, vol.50, no.1, pp.139-150,1972.
4. Keller, J.B., "Geometrical theory of diffraction", *J. Opt. Soc. Am.*, vol.52, pp.116-130,1962.
5. Srikanth, S., P.H.Pathak and C.W.Chuang, "Perfectly conducting semicircular cylinder", *IEEE Trans.*, vol.AP-34, no.10, pp.1250-1257, 1986.
6. Burnside, W.D., C. L. Yu and R. J. Marhefka, "A technique to combine the geometrical theory of diffraction and the moment method", *IEEE Trans.*, vol. AP-23, no. 6, pp. 551-558, 1975.
7. Mullar, R. F., "Singularities of two-dimensional exterior solution of the Helmholtz equation", *Proc. Cambridge Phylos. Soc.*, vol. 69, pp. 175-188, 1971.
8. Van der Berg, P. M. and J.T.Fokkema, "The Reyleigh hypothesis in the theory of refraction by a grating", *J.Opt. Soc. Am.* , vol. 69, pp. 27-31, 1979.

9. Ikuno, H. and K.Yasuura, "Improved point matching method with applications to scattering from a periodic surface", *IEEE Trans.*, vol. AP-21, no. 5, pp. 657-662, 1973.
10. Ikuno, H. and K.Yasuura, "Numerical calculation of the scattered field from a periodic deformed cylinder using the smoothing process on the mode-matching method", *Radio Science*, vol.13, no. 6, pp. 937-946, 1978.
11. Okuno, Y. and K.Yassuura, "Numerical algorithm based on the mode-matching method with a singular-smoothing procedure for analyzing edge-type scattering problems", *IEEE Trans.*, vol.AP-30, no. 4, pp. 580-587, 1982.
12. Okuno, Y. and T.Matsuda, "The mode matching method with a generalized singular smoothing procedure for analyzing the edge-type scattering problem with several edge points", *Radio Science*, vol. 19, no. 5, pp. 1148-1154, 1984.
13. Shafai, L., "Numerical solution of diffraction problems using the geometry of strip", *Inter. Jour. Elect.*, vol. 35, no. 1, pp. 113-119, 1973.
14. Veliev, E., V. Veremey and V. Shestopalov, "Electromagnetic wave diffraction on polygonal cylinders - new approach", *Proceedings of the 1989 URSI International Symposium on electromagnetic theory Stockholm, Sweden, August 14-17 1989*, p.p. 628-630.
15. Otsuki, T., "Reexamination of diffraction problem of a slit by a method of Fourier-orthogonal functions transformation", *J. Phys. Soc. Jap.*, vol. 41, no.6, pp.2046-2051, 1976.
16. Vavilov, V.N., E.I.Veliev and V.V.Veremey, "Electromagnetic wave diffraction by complicated cylindrical body", *The 3rd Asia-Pacific Microwave Conference, Proceedings, Tokyo, 1990*, pp. 527-530.
17. Ziolkovski, R. and J.B.Grant, "Scattering from cavity-backed apertures: The generalized dual series solution of the concentrically loaded E-pol slit cylinder problem", *IEEE Trans.*, vol.AP-35, no. 5, pp. 504-528, 1987.
18. Abramowitz, M. and I. A. Stegun, *Handbook of Mathematical Functions*, pp. 180- 190, Dover, New York. 1972.